Energy-Induced Modulation of the Kinetics of Oxidative Phosphorylation and Reverse Electron Transfer†

Carla Hekman, Akemi Matsuno-Yagi, and Youssef Hatefi*

Division of Biochemistry, Department of Basic and Clinical Research, Research Institute of Scripps Clinic, 10666 North Torrey Pines Road, La Jolla, California 92037

Received February 19, 1988; Revised Manuscript Received May 6, 1988

ABSTRACT: The kinetics of ATP synthesis by bovine heart submitochondrial particles (SMP) are modulated by the rate of energy production by the respiratory chain between two fixed limits characterized by apparent K_m^{ADP} = 2–4 μM and $V_{max} \approx 200$ nmol of ATP min^{-1} (mg of SMP protein)$^{-1}$ at low energy levels and apparent K_m^{ADP} = 120–160 μM and V_{max} = 11 000 nmol of ATP min^{-1} (mg of SMP protein)$^{-1}$ at high energy levels. These data indicate that K_m^{ADP} and V_{max} increase ~50-fold each; therefore, there is essentially no change in the catalytic efficiency of the ATP synthase complex in going from one extreme to the other. At intermediate rates of energy production, the kinetic data required introduction of a third, intermediate K_m^{ADP}. A K_m^{ADP} of 10–15 μM fitted all the data reported here and previously [Matsuno-Yagi, A., & Hatefi, Y. (1986) *J. Biol. Chem. 261*, 14031–14038]. However, this is not meant to suggest that there is a fixed intermediate K_m^{ADP}, as the transition from one fixed limit to the other may be fluid or involve more than one intermediate state. In addition, it has been shown that kinetic plots of SMP-catalyzed and ATP-driven reverse electron transfer from succinate to NAD are curvilinear and resolvable into a minimum of two apparent K_m^{NAD} values of about 20–30 and 200–300 μM. These results have been discussed in relation to the three potentially active catalytic sites of F_1-ATPase and the structure of the NADH:ubiquinone oxidoreductase complex, the curvilinear kinetics of ATP hydrolysis, and changes in K_m^{ADP} and $K_m^{P_i}$ in photophosphorylation as affected by the duration and intensity of light.

Previous work from this laboratory has demonstrated that Eadie–Hofstee plots (v/[S] versus v) of the kinetics of SMP[1]-catalyzed ATP synthesis at variable [ADP] or [P_i] are curvilinear with either succinate or NADH as the respiratory substrate (Matsuno-Yagi & Hatefi, 1985, 1986). The curvilinear plots could be analyzed for a minimum of two kinetic modes. One mode was characterized by low apparent K_m values for ADP (6–10 μM) and P_i (≤0.25 mM) and a limited capacity for ATP synthesis [apparent V_{max} ~500 nmol of ATP min^{-1} (mg of protein)$^{-1}$], and the second mode was characterized by 10-fold higher K_m values for ADP and P_i and a very high turnover capability for ATP synthesis. What modulated these kinetic modes appeared to be the rate of energy production by the respiratory chain relative to the number of functional ATP synthase molecules. When the rate of energy production relative to the number of functional ATP synthase complexes was low, ATP was produced predominantly in the low K_m–low V_{max} mode, whereas when the rate of energy production relative to the number of functional F_0F_1 complexes was high, then ATP was produced largely in the high K_m–high V_{max} mode (Matsuno-Yagi & Hatefi, 1986).

We had observed previously that, at very low rates of energy production, the kinetics of ATP synthesis at variable [ADP] could not be satisfied with a two-component analysis (Matsuno-Yagi & Hatefi, 1986). It seemed that an additional very low K_m^{ADP} was necessary for satisfactory fit of the data. In this paper, it will be shown that the kinetics of ATP synthesis at variable [ADP] must be analyzed in terms of a minimum of three K_m's for ADP. Two of these at very low and very high energy levels are fixed values, differing by ~50-fold. The third is an intermediate K_m, which must be introduced for satisfactory fit of the kinetic data and can be varied considerably without affecting the fixed low and the fixed high K_m values. In addition, data will be reported for the kinetics of ATP-driven reverse electron transfer from succinate to NAD. These data could be analyzed in terms of two apparent K_m values for NAD differing by 1 order of magnitude. The implications of these results on the mechanisms of oxidative phosphorylation and ATP-driven reverse electron transfer from succinate to NAD are discussed.

Materials and Methods

SMP were prepared from bovine heart mitochondria as previously described (Matsuno-Yagi & Hatefi, 1985). Protein concentrations were estimated by the method of Lowry et al. (1951). Oxidative phosphorylation driven by succinate, NADH, or β-hydroxybutyrate plus NAD as respiratory substrates was measured at 30 °C as before (Matsuno-Yagi & Hatefi, 1985; Hatefi et al., 1982), except that the succinate concentration employed was 5 mM. Ascorbate plus TMPD driven oxidative phosphorylation was initiated by the addition of 20 mM ascorbate and variable amounts of TMPD (0.25–1.5 mM final concentrations). The reaction times employed were 15, 3, 20, and 7 min for ATP synthesis supported by oxidation of succinate, NADH, β-hydroxybutyrate plus NAD, and ascorbate plus TMPD, respectively. Esterified ^{32}P was estimated according to Pullman (1967) as described by Stiggall et al. (1979). In all cases, control experiments demonstrated that ^{32}P esterification was linear with time throughout the periods employed in these studies. ATP-driven electron transfer from succinate to NAD was measured at 30 °C as previously described (Hatefi et al., 1982), except that bovine serum albumin

† Supported by U.S. Public Health Service Grant DK08126. This is Publication No. 5249-BCR from the Research Institute of Scripps Clinic, La Jolla, CA.

* Author to whom correspondence should be addressed.

[1] Abbreviations: SMP, submitochondrial particles; TMPD, *N*,*N*,*N*′,*N*′-tetramethyl-*p*-phenylenediamine; DCCD, *N*,*N*′-dicyclohexylcarbodiimide; $\Delta\psi$, membrane potential; F_0 and F_1, membrane sector and catalytic sector, respectively, of the ATP synthase complex.

0006-2960/88/0427-7559$01.50/0

was omitted and the concentration of ATP was maintained as given in the legends to Figures 6–8 by inclusion in the assay medium of 12.5 units/mL pyruvate kinase and 1.0 mM phosphoenolpyruvate. Respiratory inhibitors, including Seconal (0.3–0.8 mM), methyl malonate (1.0–10.0 mM), oxaloacetate (2.0–40.0 μM), and malonate (250 μM–2.0 mM), were added prior to initiation of the reactions. Methyl malonate is a competitive inhibitor of β-hydroxybutyrate dehydrogenase, and oxaloacetate and malonate are competitive inhibitors of succinate dehydrogenase. Seconal inhibits NADH oxidation at the level of complex I, and the inhibition under the conditions specified is not time dependent. Eadie–Hofstee plots of the kinetics of either ATP synthesis or NAD reduction at variable substrate concentrations were computer-analyzed as described previously (Matsuno-Yagi & Hatefi, 1986; Wong et al., 1984) for the least number of straight lines that when combined best fitted the experimental data.

Membrane potential, both static head and steady state, was monitored by measuring the absorbance change of oxonol VI at 630 minus 603 nm as previously described (Matsuno-Yagi & Hatefi, 1987). The temperature of the reaction mixture was maintained at 30 °C. The buffer employed was the same as that used for assays of oxidative phosphorylation, except that the radioactive phosphate was omitted. Respiratory inhibitors were added to the reaction mixture prior to establishing the static-head membrane potential by addition of respiratory substrate.

Methyl malonate and oxaloacetate were obtained from Sigma, ascorbate was from Calbiochem, and TMPD was from Eastman Kodak. The sources of all other chemicals were as specified previously (Matsuno-Yagi & Hatefi, 1985, 1986, 1987).

Results

Kinetics of ATP Synthesis at Low Rates of Respiration. As mentioned above, the curvilinear Eadie–Hofstee plots of the kinetics of ATP synthesis by bovine heart SMP at variable [ADP] or [P_i] could be analyzed in terms of two K_m values for each substrate, which in each case differed by ~1 order of magnitude (Matsuno-Yagi & Hatefi, 1986). When the rate of energy production by either succinate or NADH oxidation was attenuated beyond that which was attempted earlier, the results made it necessary to introduce a third apparent K_m for ADP in the range of 2–4 μM. Further attenuation of the rate of energy production decreased the contributions of the higher K_m components to the overall rate of ATP synthesis, resulting in data composed largely or entirely of this low K_m^{ADP}. These results are shown in the Eadie–Hofstee plots of Figure 1A with NADH as the respiratory substrate, Figure 1B with β-hydroxybutyrate as the respiratory substrate, and Figure 2 with succinate as the respiratory substrate. Table I shows the analysis of the data of Figures 1 and 2 in terms of three K_m components.[2] The intermediate and the high K_m's are essentially the same as those reported previously (Matsuno-Yagi & Hatefi, 1986), and the low K_m^{ADP} of 2–4 μM is that which has emerged from the data of Figures 1 and 2. In addition,

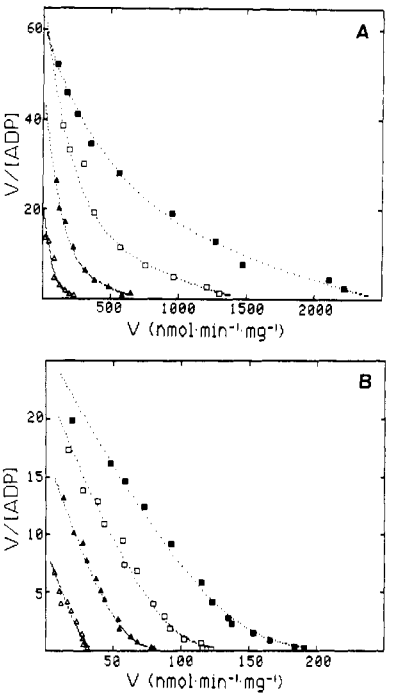

FIGURE 1: Effect of attenuation of respiration rate on the kinetics of ATP synthesis supported by NADH oxidation. Conditions for assay of oxidative phosphorylation in the presence of variable ADP concentrations (1.0–1000 μM) were as given under Materials and Methods. The respiratory substrate was 0.5 mM NADH (panel A) or 10 mM β-hydroxybutyrate plus 2.0 mM NAD (panel B). The rate of respiration was attenuated by addition to the reaction mixture in panel A of 0 (■), 0.3 (□), 0.5 (▲), and 0.8 (△) mM Seconal and in panel B of 0 (■), 1.0 (□), 3.0 (▲), and 10.0 (△) mM methyl malonate. V, nmol of ATP formed min^{-1} (mg of protein)$^{-1}$.

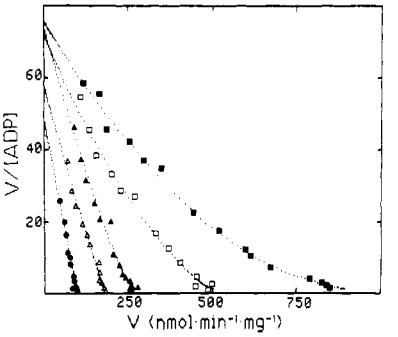

FIGURE 2: Effect of attenuation of respiration rate on the kinetics of ATP synthesis supported by succinate oxidation. Conditions for assay of oxidative phosphorylation in the presence of variable ADP concentrations (1.0–1000 μM) were the same as in Figure 1. The respiratory substrate was 5 mM succinate. The rate of respiration was attenuated by addition to the assay mixture of 0 (■), 5 (□), 10 (▲), 16 (△), and 40 (●) μM oxaloacetate. V, nmol of ATP formed min^{-1} (mg of protein)$^{-1}$.

Table I summarizes the results with ascorbate plus TMPD as the respiratory substrate. Thus, regardless of the involvement of 1, 2, or 3 coupling sites at the level of the respiratory chain, the kinetics of ATP synthesis as modulated by the rate of energy production appeared to conform to analysis in terms of three kinetic components when ADP was the variable substrate. The results shown in Figures 1 and 2 and summarized in Table I also suggested that the lowest K_m^{ADP} was a fixed value of 2–4 μM. This is apparent from the near-parallel lines in the Eadie–Hofstee plots of these figures. It was of interest, therefore, to see whether there is a fixed upper limit for K_m^{ADP}.

Kinetics of ATP Synthesis at High Rates of Respiration and High Fractional Inactivation of ATP Synthase Com-

[2] After we found that a minimum of three K_m's was necessary to accommodate the data reported here and previously (Matsuno-Yagi & Hatefi, 1986), all the Eadie–Hofstee plots for oxidative phosphorylation were analyzed in terms of three K_m values in the ranges shown in Table I. As a result, the best computer fit of the data indicated, in certain instances, very low or even negligible contribution of a kinetic component (see, for example % V_1 for V_1 in the first entry of Table I). By including such data in the tables, we do not mean that in fact these components contribute to V_t to the extent shown. The accuracy of the assays is far below such an assumption. The presentation of these marginal values simply indicates a consistent treatment of all the results.

Table I: Analysis of the Kinetics of Oxidative Phosphorylation at Variable Rates of Oxidation of NADH, β-Hydroxybutyrate, Succinate, or Ascorbate plus TMPD as the Respiratory Substrates[a]

	K_{m1}	V_1	% V_t	K_{m2}	V_2	% V_t	K_{m3}	V_3	% V_t	V_t
Respiratory Substrate: NADH										
Seconal (mM)										
0	2.6	36	1.4	15	548	22	154	1905	77	2489
0.3	2.8	125	8.5	15	259	18	158	1083	74	1467
0.5	3.2	123	17	15	103	15	155	486	68	712
0.8	3.4	54	19	10	49	17	164	181	64	284
Respiratory Substrate: β-Hydroxybutyrate										
methyl malonate (mM)										
0	3.7	66	33	9.1	73	36	161	63	31	202
1	3.0	56	42	9.7	39	30	159	37	28	132
3	2.7	42	49	13	21	25	156	22	26	85
10	2.9	24	63	10	6	16	158	8	21	38
Respiratory Substrate: Succinate										
oxaloacetate (μM)										
0	3.2	75	8.0	10.2	506	54	129	360	38	941
5	2.9	114	22	10.1	329	63	132	78	15	521
10	2.8	192	68	10.5	59	21	134	30	11	281
16	2.9	165	92	11.5	15	8	–	–	–	180
40	2.0	99	100	–	–	–	–	–	–	99
Respiratory Substrate: Ascorbate										
TMPD (mM)										
1.5	–	–	–	14.9	170	60	129	112	40	282
1.0	3.6	22	12	14.9	130	68	133	38	20	190
0.5	3.4	43	41	13.4	61	59	–	–	–	104
0.25	3.0	56	82	13.1	12	18	–	–	–	68

[a] The V_{max} (V_1, V_2, V_3) and K_m values were derived from computer analysis of the Eadie–Hofstee plots, which are shown for NADH, β-hydroxybutyrate, and succinate as respiratory substrates in Figure 1, parts A and B, and Figure 2, respectively. Conditions for assay of oxidative phosphorylation with ascorbate plus TMPD as the respiratory substrate (Eadie–Hofstee plots not shown) are given under Materials and Methods. V_t is total V_{max}, i.e., $V_1 + V_2 + V_3$, and the dashes indicate that those components did not exist in the data sets analyzed. The units for V_{max} and K_m in this and subsequent tables are nmol min^{-1} (mg of protein)$^{-1}$ and μM, respectively.

Table II: Analysis of the Kinetics of Oxidative Phosphorylation at High Rates of Respiration and High Fractional Inactivation of the F_0F_1 Complexes[a]

DCCD treatment	% remaining ATPase activity	K_{m1}	V_1	% V_t	K_{m2}	V_2	% V_t	V_t
none	100	13.6	650	24	108	2045	76	2695
16 μM, 130 min	26	12.6	112	8	126	1313	92	1425
16 μM, 200 min	13	11.4	71	7	126	918	93	989
20 μM, 165 min	10	8.6	41	5	126	716	95	757
20 μM, 210 min	6	12.4	29	5	128	526	95	555

[a] The V_{max} (V_1, V_2) and the K_m values were derived from computer analysis of the Eadie–Hofstee plots of Figure 3. V_t is total V_{max}, i.e., $V_1 + V_2$. The curve for control SMP untreated with DCCD is not shown in Figure 3.

plexes. As stated above, the conditions that favor ATP synthesis at high K_m for ADP and P_i are high rates of energy production and a limited number of functional ATP synthase complexes. The latter condition could be attained, as demonstrated elsewhere (Matsuno-Yagi & Hatefi, 1986, 1988a), by fractional inactivation of the F_0F_1 complexes with a covalently reacting inhibitor such as DCCD. When this was done, the kinetics of ATP synthesis supported by NADH oxidation became predominantly high K_m with respect to ADP (Figure 3). Furthermore, as seen in Figure 3, increasing the fractional inactivation of the F_0F_1 complexes by DCCD seemed to suggest that there is an upper limit for K_m^{ADP}. Analysis of these results (Table II) indicated essentially no contribution by the fixed low K_m^{ADP} and that the high K_m^{ADP} was ~130 μM. These results agree with those of Table I.

Thus, the totality of results presented here and elsewhere (Matsuno-Yagi & Hatefi, 1986) indicates that the kinetics of ATP synthesis by bovine heart SMP can be modulated between a low K_m^{ADP} of 2–4 μM and a high K_m^{ADP} of 120–160 μM and that one additional intermediate K_m^{ADP} must be assumed in order to satisfy all the results. At low rates of energy production relative to the number of functional ATP synthase complexes, ATP synthesis occurs in the fixed low K_m^{ADP} mode with little or no contribution from the intermediate or the high

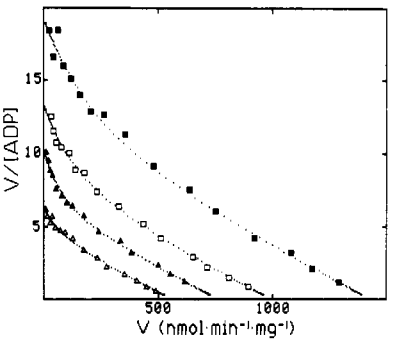

FIGURE 3: Effect of fractional inactivation of the ATP synthase complexes on the kinetics of ATP synthesis at variable concentrations of ADP. The respiratory substrate was 0.5 mM NADH. The ATP synthase complexes of SMP were inactivated to various extents by treatment of SMP at 0 °C with DCCD. The DCCD concentrations and the incubation times were as follows: (■) 16 μM and 130 min; (□) 16 μM and 200 min; (▲) 20 μM and 165 min; (△) 20 μM and 210 min; the ADP concentration range was 1.3–1100 μM. The ATPase activities of the DCCD-treated preparations were determined as described in Matsuno-Yagi and Hatefi (1984). V, nmol of ATP formed min^{-1} (mg of protein)$^{-1}$.

K_m^{ADP}. At high rates of energy production relative to the number of functional ATP synthase complexes, ATP is syn-

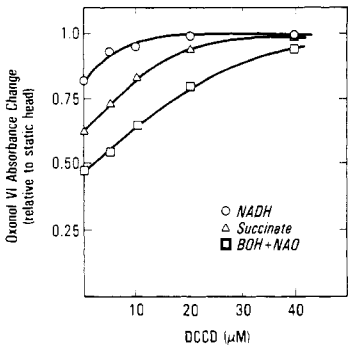

FIGURE 4: Effects of respiration rate and partial inhibition of ATP synthase by DCCD on the steady-state level of membrane potential during oxidative phosphorylation. SMP at 10 mg/mL in 0.25 M sucrose and 50 mM Tris–acetate, pH 7.5, were preincubated for ≥3 h on ice with the indicated amounts of DCCD. Oxonol VI absorbance changes were monitored as described under Materials and Methods. Static-head absorbance changes (OD) were 0.033 with NADH and succinate as respiratory substrates and 0.031 with β-hydroxybutyrate plus NAD as respiratory substrate.

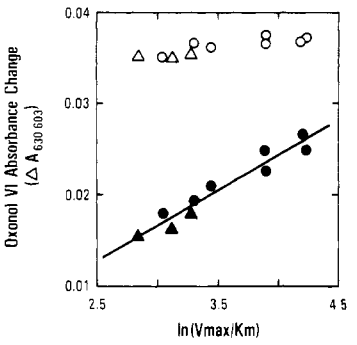

FIGURE 5: Relationship between membrane potential ($\Delta\psi$) and total V_{max}/K_m for oxidative phosphorylation at low rates of coupled respiration. Assay conditions for determination of static-head (open symbols) and steady-state (closed symbols) $\Delta\psi$ and for oxidative phosphorylation driven by 0.5 mM NADH (○, ●) or 10 mM β-hydroxybutyrate plus 2.0 mM NAD (△, ▲) are given under Materials and Methods. The rate of NADH oxidation was attenuated by addition of Seconal (0.3–0.8 mM), and the rate of β-hydroxybutyrate oxidation was attenuated by addition of methyl malonate (1.0–10.0 mM). The V_{max}/K_m values shown represent the total V_{max}/K_m values obtained from the ordinate intercepts of the appropriate Eadie–Hofstee plots with ADP as the variable substrate.

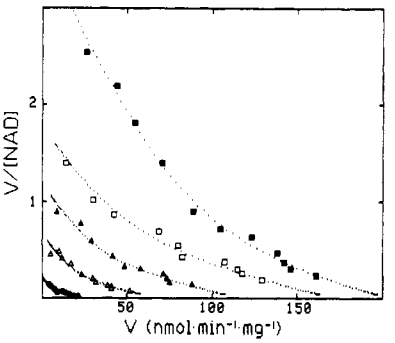

FIGURE 6: Effect of partial inhibition of complex I on the kinetics of ATP-driven electron transfer from succinate to NAD. The assay conditions at variable NAD concentrations (20–700 μM) and 0.1 mM ATP were as given under Materials and Methods. The rate of electron transfer was attenuated by addition to the assay mixtures of 0 (■), 0.05 (□), 0.10 (▲), 0.20 (△), or 0.40 (●) mM Seconal. V, nmol of NAD reduced min^{-1} (mg of protein)$^{-1}$.

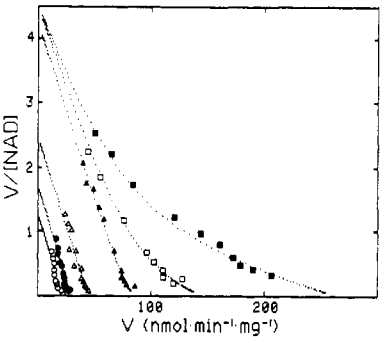

FIGURE 7: Effect of partial inhibition of succinate dehydrogenase by malonate on the kinetics of ATP-driven electron transfer from succinate to NAD. Assay conditions were the same as in Figure 6, except that the rate of electron transfer was attenuated by addition to the assay mixtures of 0 (■), 0.25 (□), 0.50 (▲), 1.0 (△), 1.5 (●), or 2.0 (○) mM malonate. V is the same as in Figure 6.

thesized essentially in the fixed high K_m^{ADP} mode with little or no contribution from the lower K_m^{ADP} modes. In between these extremes, the fixed high, the fixed low, and an intermediate K_m^{ADP} must be utilized to satisfy the experimental results, and the degree of contribution of each K_m^{ADP} to the overall kinetics of ATP synthesis depends on the rate of energy production by the respiratory chain and the number of functional ATP synthase complexes involved. For the intermediate K_m^{ADP}, one could employ a value slightly below 10 μM or as high as 40 μM with very little effect on the calculated values for the fixed low and the fixed high K_m^{ADP}. Thus, the intermediate K_m values shown in Tables I and II are arbitrary numbers introduced for best fit of the data points. This is understandable, because the extent of contribution of the low and the high K_m^{ADP} components to the overall rate of ATP synthesis is difficult to estimate. Therefore, depending on the extent assumed for the contribution of these two fixed K_m components to the overall rate of ATP synthesis, the intermediate K_m^{ADP} derived from analysis of the data can vary considerably. To conform to our previous results [see Table I in Matsuno-Yagi and Hatefi (1986)], the intermediate K_m^{ADP} employed for calculation of the present results was 10–15 μM. It should be pointed out, however, that by the above explanation we do not imply that there is a fixed intermediate K_m^{ADP}. Indeed, the transition between the two fixed limits may well be fluid.

Effects of Respiration Rate and Fractional Inactivation of ATP Synthase Complexes on Steady-State $\Delta\psi$. Increases in the coupled rate of respiration elevate the steady-state level of $\Delta\psi$ up to the capacitance limit of the SMP under consideration. Once this limit is reached, further increases in the rate of respiration will increase the rate of ATP synthesis (apparently at a lower P/O value), but with marginal effect on steady-state $\Delta\psi$. However, this steady-state $\Delta\psi$ can still be increased up to the level of static-head $\Delta\psi$ (148 ± 6 mV for our preparations of SMP; Matsuno-Yagi & Hatefi, 1987) by fractional inactivation of the ATP synthase complexes [Figure 4; see also Matsuno-Yagi and Hatefi (1987)]. Under these conditions, the synthetic turnover rate of the remaining, active ATP synthase complexes increases up to a maximum rate of 440 mol of ATP (mol of F_1)$^{-1}$ s^{-1} for bovine heart SMP at 30 °C. In addition, our data indicate that so long as steady-state $\Delta\psi$ is relatively constant, V_{max}/K_m (the ordinate intercepts of the Eadie–Hofstee plots) remains unchanged, and when $\Delta\psi$ falls, so does V_{max}/K_m. Indeed, as seen in Figure 5, there appears to be a straight-line relationship between steady-state $\Delta\psi$ and ln (V_{max}/K_m) [for further discussion of this point, see Hatefi et al. (1982) and Matsuno-Yagi and Hatefi (1988b)].

Kinetics of ATP-Driven Reverse Electron Transfer from Succinate to NAD. It was of interest to see whether the reversal of oxidative phosphorylation driven by ATP hydrolysis

Table III: Analysis of the Kinetics of ATP-Driven Reverse Electron Transfer from Succinate to NAD As Modulated by Partial Inhibition of Complexes I and II and Variable Rates of ATP Hydrolysis[a]

	K_{m1}	V_1	% V_t	K_{m2}	V_2	% V_t	V_t
Seconal (mM)							
0	25	81	39	330	124	61	205
0.05	31	43	25	310	129	75	172
0.10	30	28	24	330	89	76	117
0.20	29	15	23	320	51	77	66
0.40	24	4	15	340	23	85	27
malonate (mM)							
0	19	71	27	240	193	73	264
0.25	19	81	56	250	63	44	144
0.50	18	76	89	230	9	11	85
1.0	18	45	100	–	–	–	45
1.5	17	30	100	–	–	–	30
2.0	17	22	100	–	–	–	22
ATP (μM)							
200	20	107	28	240	273	72	380
100	19	74	29	240	186	71	260
50	20	60	34	240	119	66	179
25	18	33	36	250	59	64	92
12.5	19	13	32	240	28	68	41

[a] The V_{max} (V_1, V_2) and the K_m values for the top, middle, and bottom sections were derived from computer analysis of the Eadie–Hofstee plots shown in Figures 6–8, respectively. V_t is total V_{max}, i.e., $V_1 + V_2$, and dashes denote the absence of those components in the data sets analyzed.

would also exhibit curvilinear kinetics. As seen in Figures 6 and 7, curvilinear kinetics, resolvable into a minimum of two components, were observed with ATP-driven uphill electron transfer from succinate to NAD. Partial inhibition of complex I (NADH:ubiquinone oxidoreductase complex) by Seconal favored the conversion of the low K_m^{NAD} mode to the high K_m^{NAD} mode (Figure 6), and partial inhibition of succinate oxidation by malonate converted the high K_m^{NAD} to the low K_m^{NAD} mode (Figure 7). These modality changes are analogous to those of the kinetics of ATP synthesis when, respectively, the ATP synthases and the respiratory chain were partially inhibited [see above and Matsuno-Yagi and Hatefi (1987)]. Analysis of the data of Figures 6 and 7 is shown in Table III. It is seen (a) that K_m^{NAD} values in the two modes differ by 1 order of magnitude and (b) that the low K_m^{NAD} of 20–30 μM appears to represent a fixed lower limit for K_m^{NAD} (see Figure 7).

In oxidative phosphorylation, the kinetics of ATP synthesis are affected by the levels of two sets of substrates, i.e., ADP/P_i and protonic energy. In uphill electron transfer from succinate to NAD, there are three such substrates involved, namely, NAD, protonic energy, and electrons from succinate. As seen above, partial inhibition of the enzymes concerned with NAD reduction and succinate oxidation altered the kinetics of NADH production as expected. Partial inhibition of the enzyme (complex I) concerned with product formation converted the kinetics toward high K_m^{NAD} (Figure 6), and partial inhibition of the enzyme (succinate dehydrogenase) concerned with producing a substrate (electron) utilized by complex I for NAD reduction favored a change toward low K_m^{NAD} kinetics (Figure 7). However, diminution of the rate of ATP hydrolysis by the use of suboptimal ATP concentrations or by fractional inactivation of the F_0F_1 complexes with DCCD decreased the rate of NAD reduction without changing the contributions of the low and the high K_m^{NAD} modes to the overall kinetics of the reaction (Figure 8 and Table III). The reason for this difference may be related to changes in the rate-determining steps in NAD reduction as affected by (a) the rate of energy production by ATP hydrolysis versus (b) the rate of electron production by succinate oxidation. However, in one respect at least, perturbations of the latter two processes had a similar effect on the kinetics of NAD reduction. Both partial inhibition of ATP hydrolysis and severe inhibition of succinate oxidation decreased V_{max}/K_m (ordinate intercepts in Figures 7 and 8) for NAD reduction.

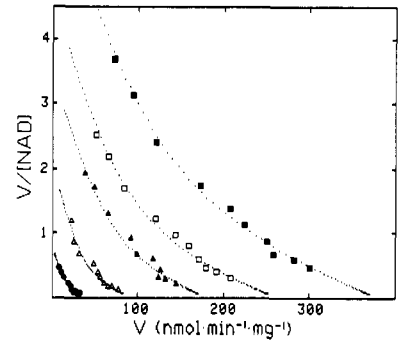

FIGURE 8: Effect of various concentrations of ATP on the kinetics of ATP-driven electron transfer from succinate to NAD. Assay conditions were the same as in Figure 6, except that the rate of electron transfer was controlled by using the following micromolar ATP concentrations: 200 (■), 100 (□), 50 (▲), 25 (△), and 12.5 (●). V is the same as in Figure 6. Similar results were obtained when, instead of lowering ATP concentration, the rate of ATP hydrolysis was diminished by fractional inactivation of the ATP synthase complexes with DCCD (data not shown).

Discussion

The data presented here and elsewhere (Matsuno-Yagi & Hatefi, 1986) indicate that the rate of energy production by the respiratory chain modulates the kinetics of ATP synthesis by SMP in the following manner. At low rates of coupled respiration, ATP is synthesized at a low rate with an apparent K_m^{ADP} = 2–4 μM. At very high rates of coupled respiration, and especially when steady-state membrane potential is increased by fractional inactivation of the ATP synthase complexes, ATP is synthesized at very high rates (V_{max} = 440 mol of ATP s^{-1} (mol of F_0F_1)$^{-1}$; Matsuno-Yagi & Hatefi, 1988a) with an apparent K_m^{ADP} = 120–160 μM. At intermediate rates of energy production, the kinetic data at variable [ADP] are curvilinear and require analysis in terms of a minimum of three K_m^{ADP}, the two fixed K_m^{ADP} values indicated above plus an intermediate K_m^{ADP}. The intermediate K_m^{ADP} of 10–15 μM employed here and previously (Matsuno-Yagi & Hatefi, 1986) fitted all the kinetic plots. However, as stated earlier, a value slightly less than 10 μM or greater than 30 μM could also be employed for the intermediate K_m^{ADP}. The only thing that changed with the use of a somewhat different intermediate K_m^{ADP} was the extent of contribution of the low and high

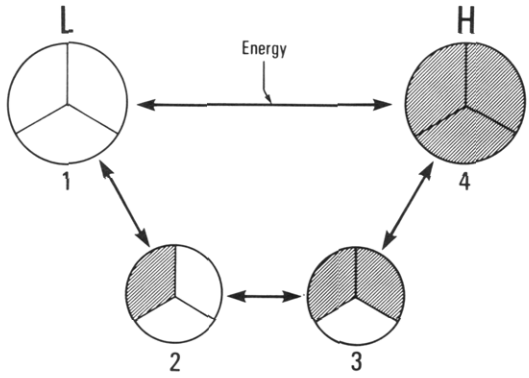

FIGURE 9: A hypothetical scheme showing energy-promoted change in the three potential catalytic subunits of F_1-ATPase. Circles marked 1 and 4 represent respectively the fixed low K_m–low V_{max} and the fixed high K_m–high V_{max} states of the enzyme, and circles marked 2 and 3 represent the states of the enzyme predominant at intermediate energy levels. Shaded areas indicate energy-induced change of a catalytic subunit to a kinetically different state.

K_m^{ADP} components to the overall rate of ATP synthesis.

In the studies reported previously (Matsuno-Yagi & Hatefi, 1986), two apparent K_m values were presented for P_i ($\leq$0.25 and $\sim$2.0 mM). There may also be a third, very low $K_m^{P_i}$ at very low rates of energy production. However, unlike ADP, which is regenerated in oxidative phosphorylation assays, P_i is consumed in these experiments. Therefore, our experimental conditions precluded a search for a very low $K_m^{P_i}$. Junge (1987) has reported values for K_m^{ADP} and $K_m^{P_i}$ of 3 and 14 μM, respectively, in photophosphorylation under conditions of flashing light and transient proton flow [see also Stroop and Boyer (1985)]. Under continuous light, $K_m^{P_i}$ was 240 μM (Junge, 1987) or higher (Aflalo & Shavit, 1983), and K_m^{ADP} under continuous high light intensity was close to 60 μM (Vinkler, 1981). The low and the high K_m^{ADP} values for photophosphorylation, respectively, under low and high levels of light energy clearly correspond to the K_m^{ADP} values reported here for oxidative phosphorylation at low and high rates of coupled respiration. Therefore, it is reasonable to assume comparable energy-dependent changes for $K_m^{P_i}$ in the two systems and a similar underlying mechanism for the kinetic modality changes in oxidative and photosynthetic phosphorylation. Furthermore, the same mechanistic principle may apply to the kinetic data presented here for ATP-driven uphill electron transfer from succinate to NAD. A possible mechanism that would satisfy these observations might be as follows.

In oxidative phosphorylation, we have shown that the kinetics of ATP synthesis are modulated by the rate of energy production between two extreme limits. When the rate of energy production relative to the number of functional F_0F_1 complexes is high, K_m^{ADP} = 120–160 μM, and the turnover capability of the ATP synthases (TN) is 440 s^{-1}, which corresponds to 11 000 nmol of ATP min^{-1} (mg of SMP protein)$^{-1}$ (Matsuno-Yagi & Hatefi, 1988a). At the other extreme, i.e., when the rate of energy production relative to the number of functional ATP synthases is low, K_m^{ADP} = 2–4 μM, and the highest rate of ATP synthesis suggested by our data is $\sim$200 nmol of ATP min^{-1} (mg of SMP protein)$^{-1}$ (Figure 2, third curve down, and Table I, third entry under succinate). Should this rate be close to the TN for the low-energy extreme, then the results suggest that TN/K_m^{ADP} remains essentially unchanged in going from the low-energy extreme to the high-energy extreme. The apparent K_m^{ADP} increases $\sim$50-fold in this transition, so does the apparent V_{max} for ATP synthesis. Thus, one could assume that, either directly or by altering the affinity of a modulator, energy regulates the kinetics of ATP synthesis between a low K_m–low V_{max} mode and a high K_m–high V_{max} mode, while V_{max}/K_m remains unchanged. However, since F_1 contains three potentially active catalytic sites, there may be intermediate states as well (see Figure 9). In that case, the kinetics of ATP synthesis at extremes of energy would be characterized by a single K_m (for ADP and P_i) and a single V_{max}, but at intermediate energy levels, the kinetics of ATP synthesis would involve the participation of two or more states of the enzyme. This interpretation is fully consistent with our results. As it is customary in dealing with curvilinear kinetic data (Cleland, 1970; Reilly et al., 1980; Sinjorgo et al., 1984), we have assumed that the curvilinearity of the kinetic plots is the result of ATP synthesis by two or more ATP synthase enzymes, each having its own K_m for ADP and P_i and its own turnover rate. Then, we have analyzed the data for the least number of such catalytic units (i.e., the least number of K_m and V_{max} values) that would give a satisfactory fit (Matsuno-Yagi & Hatefi, 1986). At one or the other energy extreme, essentially a single low or high K_m^{ADP} and a single low or high V_{max} satisfied the kinetic data, while at intermediate energy levels the data required introduction of at least one more K_m^{ADP} and V_{max}. This third K_m^{ADP} and V_{max} may be considered to represent states 2 and 3 shown in Figure 9, whose K_m^{ADP} and V_{max} values may not be too different, and depending on the level of energy, the population of one of these two intermediate states may be larger or smaller than the other. As might be expected from such a system, only two K_m^{ADP} and V_{max} values were sufficient near each extreme, either the low and the intermediate K_m^{ADP} and their associated V_{max} values or the high and the intermediate K_m^{ADP} and their associated V_{max} values (Tables I and II).

This interpretation is also in accord with the biphasic kinetics of NAD reduction by ATP-driven reverse electron transfer. Whether complex I in the mitochondrial inner membrane is monomeric or oligomeric is not known. However, it is clear that each complex I monomer contains a single primary NADH dehydrogenase and a single FMN per mole (Hatefi, 1985; Leonard et al., 1987; Ragan, 1987). Therefore, at any given energy level, there might be only one (at either energy extreme) or two (at intermediate energy levels) forms of the enzyme.

The mechanism depicted in Figure 9 is easily reconciled with the curvilinear kinetics observed in ATP hydrolysis by F_1 (Cross et al., 1982; Gresser et al., 1982). At [ATP] $\leq {}^1/_3[F_1]$, ATP is very tightly ($K_a \geq 10^{12}$ M^{-1}) bound to and very slowly hydrolyzed ($V = 1 \times 10^{-4}$ s^{-1}) by a single catalytic site per F_1 (Grubmeyer et al., 1982). At high ATP concentrations, the rate of ATP hydrolysis increases up to 10^6-fold and the apparent K_m^{ADP} is $\sim$200 μM. These results clearly indicate that additional ATP binding by F_1 increases both the apparent K_m and V_{max} for ATP hydrolysis [Cross et al., 1982; see also Wong et al. (1984)]. We have shown elsewhere (Hatefi et al., 1982; Matsuno-Yagi & Hatefi, 1988b) that SMP membrane energization increases the binding energy for both ADP and P_i. Thus, it is conceivable that just as additional ATP binding to F_1 or SMP-bound F_1 increases K_m^{ATP} and V_{max} for ATP hydrolysis (Cross et al., 1982; Penefsky, 1985), energy-promoted ADP and P_i binding to F_1 also increases K_m^{ADP}, $K_m^{P_i}$, and V_{max} for ATP synthesis.

ACKNOWLEDGMENTS

We thank Dr. C. E. Grimshaw for fruitful discussions and C. Munoz for the preparation of mitochondria.

REFERENCES

Aflalo, C., & Shavit, N. (1983) *FEBS Lett. 154*, 175–179.

Cleland, W. W. (1970) *Enzymes (3rd Ed.) 2*, 1–65.
Cross, R. L., Grubmeyer, C., & Penefsky, H. S. (1982) *J. Biol. Chem. 257*, 12101–12105.
Gresser, M. J., Myers, J. A., & Boyer, P. D. (1982) *J. Biol. Chem. 257*, 12030–12038.
Grubmeyer, C., Cross, R. L., & Penefsky, H. S. (1982) *J. Biol. Chem. 257*, 12092–12100.
Hatefi, Y. (1985) *Annu. Rev. Biochem. 54*, 1015–1069.
Hatefi, Y., Yagi, T., Phelps, D., Wong, S.-Y., Vik, S. B., & Galante, Y. M. (1982) *Proc. Natl. Acad. Sci. U.S.A. 79*, 1756–1760.
Junge, W. (1987) *Proc. Natl. Acad. Sci. U.S.A. 84*, 7084–7088.
Leonard, K., Haiker, H., & Weiss, H. (1987) *J. Mol. Biol. 194*, 277–286.
Lowry, O. H., Rosebrough, N. J., Farr, A. L., & Randall, R. J. (1951) *J. Biol. Chem. 193*, 265–275.
Matsuno-Yagi, A., & Hatefi, Y. (1984) *Biochemistry 23*, 3508–3514.
Matsuno-Yagi, A., & Hatefi, Y. (1985) *J. Biol. Chem. 260*, 14424–14427.
Matsuno-Yagi, A., & Hatefi, Y. (1986) *J. Biol. Chem. 261*, 14031–14038.
Matsuno-Yagi, A., & Hatefi, Y. (1987) *J. Biol. Chem. 262*, 14158–14163.
Matsuno-Yagi, A., & Hatefi, Y. (1988a) *Biochemistry 27*, 335–340.
Matsuno-Yagi, A., & Hatefi, Y. (1988b) *J. Bioenerg. Biomembr. 20*, 481–502.
Penefsky, H. S. (1985) *J. Biol. Chem. 260*, 13728–13734.
Pullman, M. E. (1967) *Methods Enzymol. 10*, 57–60.
Ragan, C. I. (1987) *Curr. Top. Bioenerg. 15*, 1–36.
Reilly, P. E. B., O'Shannessy, D. J., & Duggleby, R. G. (1980) *FEBS Lett. 119*, 63–67.
Sinjorgo, K. M. C., Meijling, J. H., & Muijsers, A. O. (1984) *Biochim. Biophys. Acta 767*, 48–56.
Stiggall, D. L., Galante, Y. M., & Hatefi, Y. (1979) *Methods Enzymol. 55*, 308–315.
Stroop, S. D., & Boyer, P. D. (1985) *Biochemistry 24*, 2304–2310.
Vinkler, C. (1981) *Biochem. Biophys. Res. Commun. 99*, 1095–1100.
Wong, S.-Y., Matsuno-Yagi, A., & Hatefi, Y. (1984) *Biochemistry 23*, 5004–5009.
Yagi, T., Matsuno-Yagi, A., Vik, S. B., & Hatefi, Y. (1984) *Biochemistry 23*, 1029–1036.

Evidence That Binding to the Carboxyl-Terminal Heparin-Binding Domain (Hep II) Dominates the Interaction between Plasma Fibronectin and Heparin†

Michael J. Benecky,* Carl G. Kolvenbach, David L. Amrani, and Michael W. Mosesson
Department of Medicine, University of Wisconsin Medical School, Milwaukee Clinical Campus, Milwaukee, Wisconsin 53233
Received January 6, 1988; Revised Manuscript Received April 21, 1988

ABSTRACT: We assessed the participation of the three known heparin-binding domains of PFn (Hep I, Hep II, Hep III) in their interaction with heparin by making a quantitative comparison of the fluid-phase heparin affinities of PFn and PFn fragments under physiologic pH and ionic strength conditions. Using a fluorescence polarization binding assay that employed a PFn affinity-purified fluorescein-labeled heparin preparation, we found that >98% of the total PFn heparin-binding sites exhibit a K_d in the 118–217 nM range. We also identified a minor (<2%) class of binding sites exhibiting very high affinity ($K_d \sim 1$ nM) in PFn and the carboxyl-terminal 190/170 and 150/136 kDa PFn fragments. This latter activity probably reflects multivalent inter- or intramolecular heparin-binding activity. Amino-terminal PFn fragments containing Hep I (72 and 29 kDa) exhibited low affinity for heparin under physiologic buffer conditions ($K_d \sim 30\,000$ nM). PFn fragments (190/170 and 150/136 kDa) containing both the carboxyl-terminal Hep II and central Hep III domains retained most of the heparin-binding activity of native PFn (K_d = 278–492 nM). The isolated Hep II domain (33-kDa fragment) exhibited appreciable, but somewhat lower (2–5-fold), heparin affinity compared to the 190/170-kDa PFn fragment. Heparin binding to the 100-kDa PFn fragment containing Hep III was barely detectable ($K_d > 30\,000$ nM). From these observations, we conclude that PFn contains only one major functional heparin-binding site per subunit, Hep II, that dominates the interaction between heparin and PFn.

Plasma fibronectin (PFn)[1] is a large soluble heterodimeric glycoprotein found in blood (Mosesson & Umfleet, 1970; Mosesson et al., 1975; Yamada, 1983). An insoluble "matrix" form of fibronectin (Fn) is also deposited in extracellular matrices and basement membranes. These proteins have been shown to mediate a variety of adhesive biological functions such as cell attachment and spreading. The various adhesive properties are correlated with the interaction of the various Fn binding domains with macromolecules found within cells, on cell surfaces, and in extracellular matrices.

† This study was supported by NIH Program Project Grant HL-28444. An abstract of this work has been presented at the XIth International Congress on Thrombosis and Haemostasis, Brussels, Belgium, July 1987 [*Thrombosis Haemostasis* (1987) *58*, 226].
* Author to whom correspondence should be addressed.

[1] Abbreviations: PFn, plasma fibronectin; Fn, fibronectin; PMSF, phenylmethanesulfonyl fluoride; PEG, poly(ethylene glycol); TBS, Tris-buffered saline; SDS-PAGE, sodium dodecyl sulfate–polyacrylamide gel electrophoresis; EDTA, ethylenediaminetetraacetic acid; Fl-heparin, fluorescein-labeled heparin; M_r, average molecular weight; K_d, dissociation constant; kDa, kilodaltons; FP, fluorescence polarization; ND, not determined; μ, ionic strength.

0006-2960/88/0427-7565$01.50/0